

In depth characterization of valuable char obtained from hydrothermal conversion of hazelnut shells to levulinic acid[#]

Domenico Licursi^a, Claudia Antonetti^a, Sara Fulignati^a, Sandra Vitolo^b, Monica Puccini^b, Erika Ribechini^a, Luca Bernazzani^a, Anna Maria Raspolli Galletti^{a*}

^a Department of Chemistry and Industrial Chemistry, University of Pisa, Via G. Moruzzi 13, 56124, Pisa, Italy. ^b Department of Civil and Industrial Engineering, University of Pisa, Largo Lucio Lazzarino 2, 56122, Pisa, Italy

*Corresponding author: anna.maria.raspolli.galletti@unipi.it

[#] This paper is dedicated to the loving memory of Dr. Sara Rapiti, who brilliantly graduated with a thesis on this topic, with great sorrow.

For the first time, the exploitation of hazelnut shells for the combined production of levulinic acid (LA) and hydrochar was investigated. The optimization of the catalytic hydrothermal treatment was performed both in autoclave and microwave reactor, approaching a maximum LA yield of ~9-12 wt%. Hydrochars recovered with high yield (~43-47 wt%) were characterized by different techniques, including elemental and proximate analysis, heating value, FT-IR, XPS, XRD, SEM-EDX, and SAA. Their “lignite-like” energetic properties make them suitable for the energy recovery within the same biorefinery plant for LA production, thus partially offsetting the cost of the entire process. Alternatively, since the synthesized hydrochars maintain high levels of oxygenated groups, they could be smartly exploited as natural sorbents for environmental applications. The proposed integrated approach makes possible to fully exploit this waste, smartly closing its biorefinery cycle in a sustainable development perspective.

Keywords: levulinic acid; hydrochar; hazelnut shells; hydrothermal carbonization; waste exploitation; biorefinery.

1. Introduction

Hazelnut represents a valuable biomass for the confectionery industry (Köksal et al., 2006) which generates a significant shell waste fraction. The composition of hazelnut shell is typical of the lignocellulosic biomass and

can be the starting material for carbohydrate- and lignin-derived biochemical and biofuels. Up to now, hazelnut shells have been widely used as a low-cost ground cover for gardens or in traditional thermochemical processes, mainly pyrolysis and gasification (Xiao et al., 2012; Vecchione et al., 2015). However, the surplus of this waste requires further exploitation routes and hydrothermal carbonization (HTC) has been proposed. HTC represents a low-cost process devoted to the targeted production of a carbonaceous solid, named “hydrochar” and is focused on the exclusive exploitation of the solid (Kambo and Dutta, 2015). In this process, biomass feedstock is dispersed in water and the slurry is heated at temperatures between 150 to 350 °C, at high pressure. Considering the solid phase, the HTC process involves dehydration, polymerization (condensation) and aromatization pathways, which determine the final chemical structure of the hydrochar, composed of condensed aromatic rings (Chen et al., 2017; Donar et al., 2016) but also of oxygenated functional groups, such as hydroxyl, carbonyl or carboxyl ones (Sevilla and Fuertes, 2009; Tsilomelekis et al., 2016). This hydrochar can be directly used as fuel but it is better exploited for new applications, such as for CO₂ sequestration, water purification from pollutants and as a soil amendment for agricultural uses (Mia et al., 2017). The use of hazelnut shells for the synthesis of carbonaceous materials by the HTC route has been already proposed by Donar *et al.* (2016), but the chemical nature of the HTC hydrochar and the transformations taking place during hydrothermal processing are not still well understood (Libra et al., 2011).

On the other hand, it is possible to selectively produce added-value chemicals from C5 and C6 carbohydrates by using different kinds of homogeneous/heterogeneous catalysts. For example, 5-hydroxymethylfurfural (5-HMF) represents the main furanic compound deriving as an intermediate of the selective hydrolysis/dehydration of the hexoses, and it can be converted into many biochemicals, which are exploitable in different applications (Antonetti et al., 2017). The hydrolysis of the C6 fraction can be shifted beyond 5-HMF, then producing levulinic acid (LA), a high value-added platform molecule that can be further upgraded to valuable biofuels and chemicals (Antonetti et al., 2016). The acid-catalyzed conversion of the pentoses gives furfural, another top value-added chemical of great industrial interest (Mariscal et al., 2016).

Hazelnut waste fractions are well-known for their high phenolic content, thus being suitable for the recovery of valuable antioxidants (Mattoni et al., 2017). In addition to this traditional exploitation possibility, the

conversion of its sugar fractions represents another very promising valorisation approach, which smartly completes the Biorefinery of this biomass. In this context, hazelnut shells were advantageously exploited by Uzuner and Cekmecelioglu (2014) for the production of fermentable sugars, to be used as valuable alternatives to synthetic sugars for bioprocessing and fermentation routes. The hydrothermal acid-catalyzed conversion of the sole hemicellulose fraction of the hazelnut shells into furfural was proposed by Demirbas (2006), but the author does not study the hydrochar uses. Furthermore, direct use for energy recovery at this hydrolysis step is certainly not advantageous, because it still includes structural carbohydrates of C6 fraction source, which can be further converted and exploited for the synthesis of levulinic acid (Antonetti et al. 2015). The sustainable production of this valuable platform chemical requires the use of low-cost or, even better, negative-value biomass feedstock (Antonetti et al., 2016; Licursi et al., 2016; Pileidis and Titirici, 2016), and the use of hazelnut shells is certainly attractive for this purpose. A preliminary investigation on the acid-catalyzed conversion of hazelnut shells for LA production has been reported very recently by Tukacset al. (2017), but the largely prevailing solid char was not considered. They found a maximum LA yield of 8.6 wt%, respect to the dried raw material, working at 170 °C for 8 h, under traditional heating, using H₂SO₄ 2M as a catalyst. Adopting single-mode MW heating 11.7 wt% maximum yield was obtained, shortening the reaction time up to 0.5 h.

In the present work, the optimization of the acid-catalyzed hydrothermal treatment of hazelnut shells to co-produce LA and hydrochar is investigated and discussed, adopting on the laboratory scale an autoclave and a microwave reactor, but also taking into account the industrial perspective, which provides an unavoidable feedstock variability for the LA continuous production. In this sense, the investigated biomass can be strategically mixed with other lignin-poorer feedstocks, in order to find the optimal composition for the integrated production of both LA and hydrochar. Hydrochars recovered from both optimized reactions were deeply characterized with the aim of finding possible alternative uses for the abundant waste solid obtained in the process of LA production. This approach represents a novel multivalorisation of an agri-food waste to give value added chemicals and materials (Yates et al., 2017), in a perspective of the circular economy.

2. Materials and Methods

2.1. Materials

Hazelnut shells of *Tonda Gentile Romana* variety were provided by Stelliferi-Itavex S.p.A., Caprarola, Viterbo (VT), Italy.

2.2. Methods

2.2.1. Compositional analysis

Hazelnut shells were preliminarily ball-milled and sieved, thus recovering and using the fraction with a diameter smaller than 0.84 mm. This fraction was characterized for moisture, ash, EtOH extractives, structural carbohydrates (cellulose and hemicellulose) and lignin (Klason) content, by following the official NREL procedures (Sluiter et al., 2005, 2008a, 2008b, 2008c), dried at 105 °C for 24 hours, and used in the hydrolysis tests.

2.2.2. Hydrothermal conversion

The hydrolysis experiments were carried out first by using a commercially available CEM MARS 6 multimode microwave reactor. Temperature measurement is accomplished by an immersed fiber-optic probe in one reference vessel and by two sensors located on the bottom of the reactor. Pressure measurement is achieved by an electronic sensor in the same reference vessel. Correct temperature and pressure measurements are ensured up to 300 °C and 800 psi, respectively. The maximum output power is 1800 W, but it is possible to choose lower values, when smaller amounts of reagents are used, thus avoiding overheating problems. Methods and reaction protocols can be designed as temperature/time profiles or with precise control of constant power during the reaction. The biomass (2.45 g), water (35 g) and HCl 37 wt% (1.78 g) were introduced into the reactor, then it was closed and irradiated. The following experimental conditions were chosen for the LA synthesis: reaction temperature = 180 °C; ramping time = 10 minutes; microwave power = 400 W. The experiments were performed at different reaction times.

The hydrolysis reaction was also carried out also in a 600 mL Parr zirconium-made autoclave. The autoclave was controlled by means of a Parr controller 4848. The conditions adopted for the synthesis of LA and

hydrochar in the autoclave reactor was the following: biomass (24.5 g), water (350 g) and HCl 37 wt% (17.8 g), working at 180 °C with different reaction times.

In both reaction systems, after the hydrothermal treatment, the recovered slurry was filtered under vacuum on a Büchner funnel and the isolated hydrochar was washed with fresh water, up to neutrality of pH.

2.2.3. GC-MS analysis of the hydrolysate solution

1 mL of the solution was acidified with 1 mL of HCl 6M and then extracted with diethyl ether (600 µL, three times), dried under nitrogen flow and redissolved in 1 mL of Et₂O. 200 µL of the obtained organic phase were dried under nitrogen flow and derivatized for GC/MS analysis, adding 5 µL of internal standard (tridecanoic acid in acetone) and 20 µL of derivatizing agent N,O-bis(trimethylsilyl)trifluoroacetamide (BSTFA). The reaction took place at 60 °C for 30 minutes in 150 µL of isooctane. 10 µL of the injection internal standard (hexadecane in isooctane) were added before injection in GC/MS (2 µL).

Chromatographic separation was performed with a chemically bonded fused-silica capillary column HP-5MS (Agilent Technologies, Palo Alto, CA, USA), stationary phase 5% phenyl–95% methylpolysiloxane (0.25 mm internal diameter, 0.25 µm film thickness, 30 m length), connected to 2 m × 0.32 mm internal diameter deactivated fused silica pre-column. The carrier gas was helium (99.995% purity) at a constant flow of 1.2 mL/min. The chromatographic conditions for the separation of silylated compounds were as follows: starting temperature 80 °C, isothermal for 2 min, 10 °C/min. up to 200 °C, isothermal for 3 min, 10 °C min⁻¹ up to 280 °C, isothermal for 3 min., 20 °C/min. up to 300 °C, isothermal for 20 min. Chromatograms were recorded in TIC mode (Total Ion Current, mass range 50–600). 6890N GC system gas chromatograph (Agilent Technologies) coupled with a 5975 mass selective detector (Agilent Technologies) single quadrupole mass spectrometer and equipped with PTV injector, were used. The mass spectrometer was operated in the EI positive mode (70 eV). The MS transfer line temperature was 280 °C, the MS ion source temperature was kept at 230 °C, and the MS quadrupole temperature was kept at 150 °C.

2.2.4. Quantitative determination of organic acids by High-Performance Liquid Chromatography (HPLC)

Quantitative determination of the compounds of interest was carried out by a high-performance liquid chromatograph Perkin Elmer Flexar Isocratic Platform, equipped with a column Benson 2000-0 BP-OA (300 mm × 7.8 mm), kept at 60 °C, and employing 0.005 M H₂SO₄ as mobile phase (flowrate, 0.6 mL/min). Calibration curves were acquired by adopting commercial standards of the compounds of interest. At least three replicates for each concentration of standard were carried out. The reproducibility of the technique was within 2%. The yield in LA and FA was calculated with respect to the weight of the raw biomass, as follows:

$$LA/FA \text{ Yield (\%wt)} = [LA/FA \text{ recovered after reaction (g)} / \text{dried biomass (g)}] \times 100$$

The yield of LA based on theoretical yield was calculated as follows:

$$(\%) \text{ of the theoretical LA Yield} = [LA \text{ recovered after reaction (g)} / (\text{dried biomass (g)} \times \text{cellulose content} \times 0.7155)] \times 100$$

Lastly, hydrochar yield was calculated as follows:

$$\text{Hydrochar yield (wt\%)} = [\text{dried hydrochar recovered (g)} / \text{dried starting biomass (g)}] \times 100$$

2.2.5. Elemental analysis

Samples were characterized by elemental analysis for the quantification of C, H, N and O content, by using an automatic analyzer LECO TruSpec. Carbon and hydrogen contents were determined by the infrared spectroscopy detector, whilst the nitrogen content was quantified by the thermal conductivity detector. Lastly, the oxygen content was determined by difference: O (%) = 100 (%) – C (%) – H (%) – N (%).

2.2.6. Energetic properties

Higher heating value (HHV) was determined according to the UNI EN 15400:2011 procedure, by using a home built isoperibol calorimeter, equipped with a standard Berthelot-Mahler calorimetric bomb, whose inner volume was about 400 cm³. The weighted sample (about 0.5 g) was put in a nickel-chromium alloy crucible inside the calorimetric bomb and a fusible wire, necessary for the ignition, was passed through the sample and connected to the ignition circuit. The sample was combusted in an excess of pure oxygen (about 10 bars), at constant volume (HHV_v). The bomb itself was immersed in a stirred water bath (exactly 2250 cm³ of water) within a calorimetric vessel which, in turn, was placed into an air circulating thermostat, working at room temperature. The temperature of the water bath was measured by a Pt100 probe, which was connected to an automatic resistance bridge (mod. Tinsley Senator) and the calorimetric isoperibol curve was directly acquired by a PC. The calorimeter was previously calibrated by the combustion of a certified reference of benzoic acid, thus obtaining the effective heat capacity of the instrument. Each calorimetric curve was deconvoluted, in order to obtain the thermal jump, corrected for heat losses. The global accuracy of the experimental apparatus was tested by the combustion of samples of sucrose and naphthalene and it was found better than 1%, with a reproducibility better than 0.5%. On the basis of the acquired HHV data, energy densification ratio was calculated using the following equation:

$$\text{Energy densification ratio} = \text{HHV of dried hydrochar} / \text{HHV of dried raw biomass}$$

The energy yield of the hydrochar was calculated as:

$$\text{Energy yield (\%)} = \text{hydrochar yield (\%)} \times \text{energy densification ratio}$$

2.2.7. Proximate analysis

Proximate analysis was carried out by using a thermogravimetric balance Q500 TA INSTRUMENTS. 12±1 mg of sample were weighed and heated for the determination of moisture and volatile matter, by adopting the following program: from 30 °C up to 900 °C at 20 °C/min., under nitrogen flow (100 % v/v). Then, the

sample was cooled down from 900 °C up to 800 °C, under a flow of nitrogen (40 % v/v) – air (60 % v/v), for the determination of fixed carbon and ash.

2.2.8. FT-IR analysis

FT-IR characterization of the starting biomass and its hydrolysis residues was performed by a PerkinElmer “*Spectrum-Two*” spectrophotometer. IR spectra of the samples were acquired by the KBr pellet technique, maintaining the same sample concentration (1.5 mg sample + 180 mg KBr) and thickness of each pellet ($200 \pm 10 \mu\text{m}$). The acquisition of each spectrum has provided 12 scans with a resolution of 8 cm^{-1} . The acquired spectra were normalized to 100 % of transmittance.

2.2.9. XPS analysis

X-ray photoelectron spectroscopy (XPS) measurements were conducted with an XR3E2 (VG Microtech) twin anode X-ray MgK α source (emission: 15 mA, voltage: 15 kV) and a hemispherical electron energy analyzer (HA100 from VSW Scientific Instruments).

2.2.10. XRD analysis

X-ray diffraction of the hydrochar samples was carried out by a D8 Advance Bruker instrument. The analyses were performed using the CuK radiation. The interval used was $10^\circ < \theta < 80^\circ$, with steps of 0.2° . The count of intensity was carried out every 2 s.

2.2.11. SEM-EDX analysis

Samples were viewed in a Zeiss EVO® MA 10 (Carl Zeiss NTS GmbH, Oberkochen, Germany) scanning electron microscope (SEM). An energy dispersive X-ray spectrophotometer (EDX) Link Isis-200 (Oxford Instruments, Bucks, England) operated at 10 kV coupled to the microscope was used to obtain semi-quantitative elemental compositions of selected locations of the samples, with an analyzed area of about $1 \times 1 \text{ mm}^2$.

2.2.12. Brunauer-Emmett-Teller (BET) Specific Surface Area Analysis

A single point ThermoQuest Surface Area Analyzer Qsurf S1 was used. Before the measurement, the sample was treated at 130 °C for 12 hours under a nitrogen flow of 35 mL/min. Subsequently, the sample was cooled down to the temperature of the liquid nitrogen (77K) for the measurement.

3. Results and Discussion

3.1. Compositional analysis

Compositional analysis of the starting hazelnut shells is reported in Table1 on adry basis (moisture content equal to 5.1 wt%):

Table 1, near here

The above data show a prevailing contribution of lignin (37.6 wt %), whilst hemicellulose (23.5 wt%) and cellulose (22.9 wt%) fractions are less abundant and almost equally distributed, in agreement with the results reported in the literature for this kind of biomass (Demirbas, 2002). Regarding the C5 fraction, the prevailing presence of xylose was ascertained, together with less amount of arabinose, whilst mannose, galactose, and rhamnose were absent, in agreement with a structure of the hemicellulose of glucuronoxylan type. The high lignin content is an advisable prerequisite for the exploitation of this waste biomass as starting feedstock not only for thermochemical routes but also for the hydrothermal conversion (Haykiri-Acma et al., 2010). The low ash content of hazelnut shells is important for the hydrothermal route, due to possible salt precipitation, depending on the adopted acid catalyst.

3.2. Hydrothermal conversion

Two different approaches for the synthesis of the hydrochars can be adopted, e.g. *i*) the acid-catalysed hydrothermal treatment, where the hydrochar is recovered after furfural and levulinic acid production and *ii*) the biomass carbonization in the absence of acid (HTC), which produces the hydrochar after solubilization of the C5 and C6 carbohydrates in the liquid phase. A scheme of these different paths is reported in Figure 1:

Figure 1, near here (2-column)

HTC route (Path B in Figure 1) is focused on the exclusive exploitation of the final solid hydrochar, whilst the liquid fraction, which should include C5 and C6 soluble oligomers/monomers and their degradation products, is not considered.

On the other hand, it is possible to use an acid catalyst, which is able to dehydrate/hydrolyse the C5/C6 fractions of the biomass to furfural and LA, respectively (path A, in Figure 1). The reaction conditions, mainly temperature and time, can be properly tuned for selectively obtaining both these bioproducts in cascade (path A1, in Figure 1), e.g. firstly mild reaction conditions allow the synthesis of FUR, and secondly harsher ones allow the production of LA. The hydrochar should be always recovered after the 2nd hydrolysis step, after LA synthesis (Licursi et al., 2015) when also hexoses have been exploited and the solid residue includes much more reactive functional groups, deriving both from the contribution of the lignin units of the biomass, and from that of humins, the latter formed by condensation reactions of furan intermediates, 5-HMF and furfural, originated from C6 and C5 sugar conversion, respectively. In this perspective, the one-pot hydrolysis to give LA (path A2 in Figure 1) appears more suitable for obtaining a more “reactive” hydrochar, including the functional groups of the furanics (furfural and 5-hydroxymethylfurfural) which are not separated from the lignin-rich solid but rather integrated with it by condensation reactions. In addition, the “one-pot” approach A2 corresponds to the approach adopted for the industrial production of LA from different raw biomasses on a commercial scale (GF Biochemicals, 2017). The reaction conditions for A2 path have been chosen by taking into account our previous results on different lignocellulosic raw materials (Antonetti et al., 2015; Licursi et al., 2015). Two different heating systems were compared (conventional and microwave), employing the same biomass loading, acid concentration, and reaction temperature, but different reaction times. HCl was preferred catalyst for this reaction because H₂SO₄ can cause precipitation of insoluble salts during the hydrothermal processing, which can cause clogging of the reactor, whilst the use of HCl greatly reduces this problem (Raspolli Galletti et al., 2012). In addition, hydrochloric acid allows easy recovery by atmospheric/vacuum distillation and steam stripping, 95% of the acid catalyst being recycled after LA production (Antonetti et al., 2015). The reaction was considered optimized when both glucose and fructose were no more detected in the liquid phase, evaluating the effect of the different heating on the properties of the “best” hydrochar produced, not prolonging the degradation of the residual solid more than necessary. The GC-MS analysis of the hydrolysate solution has confirmed the prevailing presence of LA,

together with less abundant compounds, including mainly guaiacol, syringol, vanillin, vanillic and gallic acid, which are markers of lignin source.

The results of the hydrolysis tests are reported in Table 2.

Table 2, near here

These data underline that MW irradiation represents a fast and efficient system for the contemporary production of LA and hydrochar, allowing to reach good LA yields and significant energy and time-saving respect to the autoclave. Acetic acid was also formed, deriving from the acetyl groups released during hemicellulose hydrolysis (Table 1). The LA yield was slightly higher for the autoclave runs, probably due to the much longer thermal transients needed for system heating/cooling. The quite low cellulose content of the hazelnut shells is the reason for the limited LA yields, if these are compared with those obtained from the conversion of more cellulose-rich biomasses (Antonetti et al., 2015). On the other hand, if the yield data are expressed in terms of % of the theoretical LA yield, these are in agreement with those reported for the hydrolysis of different waste biomasses, as poplar sawdust or paper wastes (Raspolti Galletti et al., 2012), approaching ~80 % of the theoretical yield, in the best case. It is important to highlight that the achieved data correspond to the highest ones up to now obtained in this biomass conversion route (Antonetti et al., 2016).

From the perspective of the hydrochar production, with respect to the other investigated waste and herbaceous biomasses (Antonetti et al., 2015), the highest hydrochar yield was obtained from the conversion of the hazelnut shells. The hydrochars recovered from the best hydrothermal conversions in MW and autoclave reactors (MW_3 and Auto_3 in Table 2, respectively) were further characterized, as reported in the following paragraphs.

3.3. Elemental analysis

The results of this characterization are reported in Table 3, where the elemental analysis of the starting biomass is also inserted:

Table 3, near here

The hydrochar has an elemental composition significantly different from that of the starting biomass, resulting in higher carbon content and lower oxygen one. This chemical composition is very similar to that of

lignite (Düdder et al., 2016), as just observed for the hydrochar recovered after hydrolysis of herbaceous biomasses (Licursi et al., 2015), thus confirming the successful carbonization of the starting hazelnut shells. The above data can be advantageously reported as atomic ratios H/C and O/C in a van Krevelen plot for a useful visual estimation of aromaticity and oxidation state of the hydrochars, respectively (Agarwal et al., 2017, Liu et al., 2017). These data are reported in Figure 2 for the samples of interest, together with dehydration, decarboxylation, and demethylation trends.

Figure 2, near here (single column)

H/C and O/C ratios of the hazelnut shell hydrochars are within the ranges reported in the literature for this kind of carbonaceous materials (H/C: ~0.8-1.4 and O/C: ~0.3-0.5), e.g. lignite (Brown coal) (Licursi et al., 2015). This hydrochar includes both lignin degradation products (Ribechini et al., 2012), and certainly humins, which show similar atomic ratios (Rasrendra et al., 2013). This characterization confirmed the similarity between MW and autoclave approach. However, an optimal H/C ratio of hydrochars showing good aromaticity degree should be ~0.5, whilst the ascertained values were higher, thus highlighting the possible inclusion of aliphatic volatile organic C (VOCs), and/or low level of aromatic condensation during hydrochar production (Mia et al., 2017). Furthermore, the ascertained O/C ratios indicate the abundant presence of oxygenated functional groups, which are typical of very aged (artificially or naturally) biochars (Mia et al., 2017). An O/C ratio in the range 0.2-0.6 is typical of biochars which are more resistant to decay, with a longer half-life in the soil (>1000 years), due to the stable structure of its graphitic sheets (Zhang et al., 2016). Lastly, the comparison of the H/C and O/C atomic ratios of the starting hazelnut shells and those of the hydrochars confirms that dehydration represents the prevailing mechanism of this hydrochar formation, as previously observed for the giant reed hydrochar (Licursi et al., 2015).

3.4. Energetic properties

Hydrochar recovered after acid-catalyzed hydrothermal treatment of hazelnut shells could be directly used for energetic purposes, for example within the same plant for LA production. **In the adopted laboratory scale, the isolated hydrochar has maintained about 50 wt% of water. Instead, from the industrial perspective, different strategies can be adopted, in particular, those at low energy demand, such as the mechanical dewatering by a filter press, which is able to remove economically up to about 75% of initial humidity**

(Burguete et al., 2016). For this reason, the direct combustion of the hydrochar within the same LA plant is economically advantageous. Furthermore, the evaluation of the energetic properties is attractive because it integrates the results of the elemental analysis, being an indirect confirmation of the effectiveness of the hydrothermal treatment. Therefore, the energetic properties of the synthesized hydrochars, in terms of higher heating value (HHV), energy densification ratio and energy yield, were investigated and the results are reported in Table 4, together with those of the starting biomass. The energetic properties were evaluated on a dry basis, in order to standardize the experimental data independently from the different available filtration procedures.

Table 4, near here

HHV of the starting biomass is in agreement with the data reported in the literature (Demirbas, 2002; Haykiri-Acma et al., 2010). HHV of the untreated hazelnut shells is higher than that of other biomasses, such as straw and corn cobs, but rather low if compared with carbon-rich biomasses (Demirbas et al., 1997). Instead, the hydrochars recovered from the acid-catalysed hydrothermal treatment of hazelnut shells show an increased energetic content, which is comparable with that of the traditional lignite coal (Sevilla and Fuertes, 2009), thus indirectly confirming the elemental analysis results (Table 3 and Figure 2). The above data are in agreement with those reported by Licursi et al. (2015) for the giant reed (*Arundo Donax L.*) hydrochar, which was synthesized adopting similar reaction conditions.

Dehydration, decarboxylation, and condensation reactions resulted in the carbonization of the feedstock, leading to energy densification, a parameter which is used to assess the effectiveness of the hydrothermal carbonization processes. In both cases, an energy densification ratio equal to 1.3 was ascertained, this value falls within the range reported for this carbonization route (Sermyagina et al., 2015; Elaigwu and Greenway, 2016). Regarding energy yields of the synthesized hydrochars, these fall in the range ~55-60 %, being consistent with the values reported for hydrochars obtained from other feedstocks, such as rapeseed husk (Elaigwu and Greenway, 2016), walnut shell, and sunflower stem (Román et al., 2012). Higher energy yields (70-80%) can be obtained if hydrochar mass yield is higher, this depending on differences both in the composition of the starting feedstocks and in the severity of the reaction conditions adopted for the carbonization procedure (Sermyagina et al., 2015). In our case, hazelnut shells underwent a significant solubilization of structural C5 and C6 carbohydrates, this resulting in intermediate hydrochar mass yields,

offset by the simultaneous production of LA in the liquid phase, hitherto not pursued in the HTC process. From an industrial perspective, taking into account both the starting water content and the energy densification ratio of the synthesized hydrochar, it is noteworthy to underline that it is sufficient to dewater it up to a water content of about 20 wt%, in order to get a positive energy surplus, expressed as densification ratio higher than 1.

3.5. Proximate analysis

The proximate analysis data of the investigated samples are reported in Figure 3, as thermograms:

Figure 3, near here (single column)

Taking into account the thermogravimetric curves reported in Figure 3, three thermal degradation steps can be identified. The first one is due to the moisture loss of the sample (<5 wt%). The second step includes thermal degradation of the main macro-components of biomass, e.g. hemicellulose, cellulose, and lignin for the untreated biomass (Chen and Kuo, 2010). During this step, the greatest weight loss occurs, corresponding to ~75 and ~50 wt% for the untreated biomass and its hydrochars, respectively. The improved thermal stability of the hydrochars confirms their occurred carbonization, giving an estimation of the condensation degree due to the hydrothermal processing (Licursi et al., 2015). In the last step, the weight loss of the untreated biomass is lower than those of the hydrochars, amounting to ~22% vs ~45 %, respectively, being due to the contribution of the fixed C and further confirming all the above conclusions. Lastly, the lower ash content in the hydrochar suggests that a partial solubilization of these inorganics occurred, due to the acid catalyst adopted.

3.6. FT-IR spectroscopy

The FT-IR spectrum of the untreated biomass confirms the presence of both structural carbohydrates and lignin. In fact, the wide absorption band at about 3400 cm^{-1} , is due to the O-H stretching, whilst the band at 1740 cm^{-1} is due to the stretching of the C=O bonds of carboxylic, ketone and ester groups, which are present in both carbohydrates and lignin. Ring vibrations of the C=C bonds of the aromatic structures give mainly two absorption bands, at 1630 and 1515 cm^{-1} (Düdder et al., 2016). Those in the region between 1500 and 1300 cm^{-1} are mainly due to the bending vibrations of the O-H bonds and to deformation vibrations of

methyl and methylenic groups of lignin and cellulose. The absorption bands between 1300 and 1200 cm^{-1} are due to the vibrational stretching of the C-O bonds of alcoholic, phenolic and carboxylic groups. In detail, that at 1264 cm^{-1} is due to breathing vibrations, which are typical of guaiacyl units of lignin, whilst the shoulder at 1160 cm^{-1} and the band at 1031 cm^{-1} identify C-O-C bending vibrations of hemicellulose and cellulose. Lastly, the signal at 900 cm^{-1} is due to deformation vibrations of the C-H bonds of cellulose source.

FT-IR spectrum of the hydrochars recovered from both hydrothermal treatments are identical for the intensities of the bands, but their positions are different respect to that of the starting biomass, maintaining only that in the region 3000-3500 cm^{-1} , due to the stretching of the O-H bonds of carboxylic and hydroxyl groups, and those at 2934 and 2850 cm^{-1} , due to C-H stretching. Instead, the absorption band of the C=O groups is shifted from 1740 cm^{-1} (in the untreated biomass) up to 1700 cm^{-1} (in the hydrochar), in this last case being certainly due to C=O stretching vibrations of carboxylic acids or ketones (Sun and Li, 2004). The signal at 1610 cm^{-1} (due to C=C ring stretching vibrations) is much more intense in the case of the hydrochars, indicating the presence of condensed structures of the aromatic source, and confirming the biomass carbonization (Sun and Li, 2004). The presence of carbonyl and carboxyl groups is associated with the presence of lignin units but also to that of furanic derivatives, such as furfural and 5-hydroxymethylfurfural (van Zandvoort et al., 2013), which may condense together and/or with the aromatic lignin units.

Below 1430 cm^{-1} it is possible to detect some distinctive absorption bands, such as that at 1270 cm^{-1} (aryl ring bending and C-O stretching), which is typical of guaiacyl units of lignin, those at 1214 cm^{-1} (C-O stretching), and 1030 cm^{-1} (C-O stretching), which are more intense for the hydrochar than for the untreated biomass. The intense band at 1214 cm^{-1} may be due to the stretching of phenolic -OH, thus highlighting a higher content of these functional groups (Ghaffar et al., 2015). New absorption bands at 862 cm^{-1} and 808 cm^{-1} , can be found in the hydrochar, which are attributed to aromatic out-of-plane bending vibrations of C-H bonds.

The presence of these signal patterns evidences that the acid-catalyzed hydrothermal treatment produces a functionalized hydrochar, rich of oxygenated functional groups (mainly carbonyl and aliphatic/aromatic hydroxyl groups).

3.7. XPS analysis

XPS analysis can provide very useful qualitative and quantitative information about the chemical composition of the hydrochar, in terms of kinds of elements and bonding pattern, analyzing the surface up to a depth of about 10–20 nm. The acquired XPS spectra confirm the presence of carbon, with a binding energy of 286 eV, and oxygen, with a binding energy of 534 eV, thus highlighting the prevailing existence of these elements on the surface of both hydrochars, which appear analogous. In greater detail, the samples have a high amount of elemental C (79.7 % and 79.2 %, for the autoclave- and MW-hydrochars, respectively), whilst the remaining part is exclusively composed by elemental O. Peak deconvolution was carried out in order to estimate the relative proportions of the functional groups of these samples. Deconvolution of the XPS spectra of both hydrochars gave analogous results. Taking into account the deconvoluted C1s spectrum, three peaks have been identified, e.g. that at 284.6 (C-C), 286.1 (C-O-H (hydroxyl) and C-O-C (ether)), 288.0 eV (C=O (carbonyl)), together with a shoulder at 290.0 eV (O=C-O (acid or ester)) (Yu et al., 2012). Instead, deconvolution of the O1s spectrum gave two peaks, that at 532.5 (O=C) and 534.6 eV (O-C; -OH). The C and O functional group compositions derived from deconvolution of the XPS spectra are reported in Table 5, as normalized areas:

Table 5, near here

The reprocessed data highlight better the presence of very high levels of oxygenated functionalities, these belonging to humin and lignin structures on the surface, in agreement with the conclusions of the FT-IR characterization. Furthermore, the contribution to the area of the signal at 284.8 eV, which is attributed to aromatic C-C bond, is modest, especially if compared with that of different biochars (Srinivasan et al., 2015), thus supporting the idea that the investigated hydrochars have lower proportions of aromatic compounds than biochars, e.g. being less “stable”, but richer in more “reactive” oxygenated groups (Weidner et al., 2013). The low condensation degree of the investigated hydrochars is also confirmed by the absence of the signal at 291 eV ($\pi \rightarrow \pi^*$ shake-up satellites), which is typical of extended pre-graphitic polyaromatic domains (Yu et al., 2012).

3.8. XRD analysis

Hydrochars were further characterized by X-ray diffraction (XRD). The acquired diffractograms highlight the presence of a broad peak between 20 and 30°, which is ascribed to the diffraction of the amorphous carbon (Yu et al., 2012). Both synthesized hydrochars resulted composed of very disordered and amorphous structures.

3.9. SEM-EDX analysis

EDX elemental analysis data of the investigated samples are reported in Table 6.

Table 6, near here

SEM images of the starting biomass show a classical superficial microstructure, which is typical of lignocellulosic biomass. Unlike woody biomasses, which have a fibrous structure due to the abundant presence of cellulose, hazelnut shells show a very compact and recalcitrant morphology, mainly attributed to the lignin component (Haykiri-Acma et al., 2010), which is very abundant in this biomass (Table 1). Instead, SEM images of the hydrochars recovered from both hydrothermal treatments have an identical appearance, revealing the presence of spherical particles, certainly humins (Tsilomelekis et al., 2016), on the lignin substrate, the latter being variously degraded. The presence of humins seems quite clear already at low magnifications (500x), but it is better defined at much more higher magnifications (>1000x).

EDX analysis of the hydrochars confirmed their similar elemental composition, thus supporting the conclusion that the two adopted heating treatments had similar effects on the solid phase. On the other hand, the chemical composition of the hydrochars is very different from that of the untreated biomass, which shows traces of some elements of the inorganic source. EDX still allowed the detection of traces of Cl and Fe in both hydrochars, which were not identified by the XPS analysis, due to the shallower depth of analysis of this latter technique (10-20 nm and 2-4 µm for XPS and EDX, respectively). The increase in chlorine content, passing from starting biomass to both hydrochars, is certainly due to the presence of traces of trapped acid catalyst, despite thorough washings were carried out before the characterization activity. The C and O data for the hydrochars are well in agreement with those obtained by the traditional elemental analysis (Table 3), thus highlighting a homogeneous composition of the hydrochar through the entire biomaterial. Instead, the C content of the starting biomass is higher than that obtained by traditional elemental analysis

(Table 3), highlighting a more important contribution of the carbon-rich lignin fraction on the biomass surface, rather than the oxygen-rich carbohydrates, as previously stated.

3.10. Brunauer-Emmett-Teller (BET) Specific Surface Area Analysis

Specific surface area (SSA) is one of the main physical properties that may affect char sorption capacity (Rajapaksha et al., 2016). Free surface area of biochar is mainly determined by *i*) the microstructure of the starting untreated biomass (e.g. capillary structures such as xylem in woody biomass), and *ii*) the physical cracking due to mass loss and shrinkage occurred during its processing. BET surface area of the untreated shells was measured as a reference and resulted negligible, due to the remarkable contribution of the unmodified lignin, which protects the whole biomass. On the other hand, surface areas of the hydrochars recovered after hydrothermal treatment in autoclave and microwave were measured, amounting in both cases only to about $10 \text{ m}^2 \text{ g}^{-1}$. This low value is due to the partial destruction of biomass cellular structures, and the precipitation of the insoluble furanics (humins) and other reaction products, such as the same LA and FA, on the lignin surface (substrate), thus limiting the free surface and accessibility (Yu et al., 2012; Rasrendra et al., 2013). These data suggest that some physical or chemical activation post-treatments should be performed for the removal of VOCs, in order to increase the hydrochar surface area and porosity, to be tuned depending on the desired application.

4. Conclusions

The acid-catalyzed hydrothermal conversion of hazelnut shell into LA was investigated and optimized both in autoclave and microwave reactors. Good LA yields (~9-12 wt%) and very high hydrochar yields (~43-47 wt%) were ascertained. The occurred carbonization of the starting biomass was demonstrated, and the hydrochar showed a “lignite-like” behavior, certainly suitable for energy production. In order to find possible uses of the hydrochar, e.g. better understanding its reactivity, a complete characterization was carried out. From an integrated perspective of the LA process, the characterization of the hydrochar is of fundamental importance because, independently from the starting feedstock, humins are the main by-products of this reaction, then depositing on the surface of the hydrochar. The presence of these furanic compounds, hitherto considered as the main drawback of the LA process, increases the reactivity of the hydrochar, in terms of new

functional groups. Their analysis has demonstrated the feasible use of the hydrochar as an adsorbent for environmental applications. However, an activation treatment is advisable for improving its available surface area, now limited by trapped VOCs. In this regard, preliminary tests of chemical activation of the synthesised hydrochar have been carried out, achieving promising results, in terms of both surface area and porosity distribution, and this research is in progress.

Appendix A. Supplementary data

Supplementary data associated with this article can be found, in the online version, at the website.

List of abbreviations. LA: Levulinic Acid; FT-IR: Fourier Transform-Infrared Spectroscopy; XPS: X-Ray Photoelectron Spectroscopy; XRD: X-Ray Diffraction; SEM-EDX: Scanning Electron Microscopy-Energy Dispersive X-Ray Spectroscopy; SAA: Surface Area Analysis; HTC: Hydrothermal Carbonization; MW: Microwave; HPLC: High Performance Liquid Chromatography; HHV: Higher Heating Value; GLU: Glucose; FUR: Furfural; AA: Acetic Acid; FA: Formic Acid.

References

1. Agarwal, S., van Es, D., Heeres, H.J., 2017. Catalytic pyrolysis of recalcitrant, insoluble humin by-products from C6 sugar biorefineries. *J. Anal. Appl. Pyrolysis* 123, 134-143.
2. Antonetti, C., Bonari, E., Licursi, D., Nassi o Di Nasso, N., Raspolli Galletti, A.M., 2015. Hydrothermal conversion of giant reed to furfural and levulinic acid: optimization of the process under microwave irradiation and investigation of distinctive agronomic parameters. *Molecules* 20, 21232-21253.
3. Antonetti, C., Licursi, D., Fulignati, S., Valentini, G., Raspolli Galletti, A.M., 2016. New frontiers in the catalytic synthesis of levulinic acid: from sugars to raw and waste biomass as starting feedstock. *Catalysts* 6, 196-225.
4. Antonetti, C., Melloni, M., Licursi, D., Fulignati, S., Ribechini, E., Rivas, S., Parajó, J.C., Cavani, F., Raspolli Galletti, A.M., 2017. Microwave-assisted dehydration of fructose and inulin to HMF catalyzed by niobium and zirconium phosphate catalysts. *Appl. Catal. B: Environ.* 206, 364-377.

5. Burguete, P., Corma, A., Hitzl, M., Modrego, R., Ponce, E., Renz, M., 2016. Fuel and chemicals from wet lignocellulosic biomass waste streams by hydrothermal carbonization. *Green Chemistry* 18, 1051-1060.
6. Chen, W.H., Kuo, P.C., 2010. A study on torrefaction of various biomass materials and its impact on lignocellulosic structure simulated by a thermogravimetry. *Energy* 35, 2580–2586.
7. Chen, X., Lin, Q., He, R., Zhao, X., Li, G., 2017. Hydrochar production from watermelon peel by hydrothermal carbonization. *Bioresour. Technol.* 241, 236-243.
8. Demirbas, A., Gullu, D., Çağlar, A., Akdeniz, F., 1997. Estimation of calorific values of fuels from lignocellulosics. *Energy Sources* 19, 765-770.
9. Demirbas, A., 2002. Fuel characteristics of olive husk and walnut, hazelnut, sunflower, and almond shells. *Energy Sources* 24, 215-221.
10. Demirbas, A., 2006. Furfural production from fruit shells by acid-catalyzed hydrolysis. *Energy Sources, Part A* 28, 157–165.
11. Donar, Y.O., Çağlar, E., Sinağ, A., 2016. Preparation and characterization of agricultural waste biomass-based hydrochars. *Fuel* 183, 366–372.
12. Düdder, H., Wütscher, A., Stoll, R., Muhler, M., 2016. Synthesis and characterization of lignite-like fuels obtained by hydrothermal carbonization of cellulose. *Fuel* 171, 54-58.
13. Elaigwu, S.E., Greenway, G.M., 2016. Microwave-assisted hydrothermal carbonization of rapeseed husk: A strategy for improving its solid fuel properties. *Fuel Process. Technol.* 149, 305-312.
14. GFBiochemicals, 2017. <http://www.gfbiochemicals.com> (accessed 20.01.17)
15. Ghaffar, A., Ghosh, S., Li, F., Dong, X., Zhang, D., Wu, M., Li, H., Pan, B., 2015. Effect of biochar aging on surface characteristics and adsorption behavior of dialkyl phthalates. *Environ. Pollut.* 206, 502–509.
16. Haykiri-Acma, H., Yaman, S., Kucukbayrak, S., 2010. Comparison of the thermal reactivities of isolated lignin and holocellulose during pyrolysis. *Fuel Process. Technol.* 91, 759–764.
17. Kambo, H.S., Dutta, A., 2015. A comparative review of biochar and hydrochar in terms of production, physicochemical properties and applications. *Renew.Sust.Energ. Rev.* 45, 359-378.

18. Köksal, A.I., Artik, N., Simsek, A., Günes, N., 2006. Nutrient composition of hazelnut (*Corylusavellana* L.) varieties cultivated in Turkey. *Food Chem.* 99, 509–515.
19. Libra, J.A., Ro, K.S., Kammann, C., Funke, A., Berge, N.D., Neubauer, Y., Titirici, M.-M., Fühner, C., Bnes, O., Kern, J., Emmerich, K.-H., 2011. Hydrothermal carbonization of biomass residuals: a comparative review of the chemistry, processes, and applications of wet and dry pyrolysis. *Biofuels* 2, 71-106.
20. Licursi, D., Antonetti, C., Bernardini, J., Cinelli, P., Coltelli, M.B., Lazzeri, A., Martinelli, M., Raspolli Galletti, A.M., 2015. Characterization of the *Arundo Donax* L. solid residue from hydrothermal conversion: Comparison with technical lignins and application perspectives. *Ind. Crop. Prod.* 76, 1008–1024.
21. Licursi, D., Antonetti, C., Martinelli, M., Ribechini, E., Zanaboni, M., Raspolli Galletti, A.M., 2016. Monitoring/characterization of stickies contaminants coming from a papermaking plant – Toward an innovative exploitation of the screen rejects to levulinic acid. *Waste Manage.* 49, 469-482.
22. Liu, Y., Yao, S., Wang, Y., Lu, H., Brar, S.K., Yang, S., 2017. Bio- and hydrochars from rice straw and pig manure: Inter-comparison. *Bioresour. Technol.* 235, 332-337.
23. Mariscal, R., Maireles-Torres, P., Ojeda, M., Sádabaa, I., LópezGranadosa, M., 2016. Furfural: a renewable and versatile platform molecule for the synthesis of chemicals and fuels. *Energy Environ. Sci.* 9, 1144-1189.
24. Mattonai, M., Licursi, D., Antonetti, C., Raspolli Galletti, A.M., Ribechini, E., 2017. Py-GC/MS and HPLC-DAD characterization of hazelnut shell and cuticle: insights into possible re-evaluation of waste biomass, *J. Anal. Appl. Pyrolysis*, doi: 10.1016/j.jaap.2017.07.019.
25. Mia, S., Dijkstra, F.A., Singh, B., 2017. Long-term aging of biochar: A molecular understanding of agricultural and environmental implications. *Adv. Agron.* 141, 1-51
26. Pileidis, F.D., Titirici, M.-M., 2016. Levulinic acid biorefineries: new challenges for efficient utilization of biomass. *ChemSusChem* 9, 562–582.
27. Raspolli Galletti, A.M., Antonetti, C., de Luise, V., 2012. Levulinic acid production from waste biomass. *Bioresources* 7, 1824–1835.

28. Rasrendra, C.B., Windt, M., Wang, Y., Adisasmito, S., Makertihartha, I.G.B.N., van Eck, E.R.K., Meier, D., Heeres, H.J., 2013. Experimental studies on the pyrolysis of humins from the acid catalysed dehydration of C6-sugars. *J. Anal. Appl. Pyrolysis* 104, 299–307.
29. Rajapaksha, A.U., Chen, S.S., Tsang, D.C.W., Zhang, M., Vithanage, M., Mandal, S., Gao, B., Bolan, N.S., Ok, Y.S., 2016. Engineered/designer biochar for contaminant removal/immobilization from soil and water: Potential and implication of biochar modification. *Chemosphere* 148, 276–291.
30. Ribechini, E., Zanaboni, M., Raspolli Galletti, A.M., Antonetti, C., Nasso, N., Bonari, E., Colombini, M.P., 2012. Py-GC/MS characterization of a wild and a selected clone of *Arundo Donax*, and of its residues after catalytic hydrothermal conversion to high added-value products. *J. Anal. Appl. Pyrolysis* 94, 223–229.
31. Román, S., Nabais, J.M.V., Laginhas, C., Ledesma, B., González, J.F., 2012. Hydrothermal carbonization as an effective way of densifying the energy content of biomass. *Fuel Process. Technol.* 103, 78–83.
32. Sermyagina, E., Saari, J., Kaikko, J., Vakkilainen, E., 2015. Hydrothermal carbonization of coniferous biomass: Effect of process parameters on mass and energy yields. *J. Anal. Appl. Pyrolysis* 113, 551–556.
33. Sevilla M, Fuertes A.B., 2009b. Chemical and structural properties of carbonaceous products obtained by hydrothermal carbonization of saccharides. *Chem. Euro. J.* 15, 4195–4203.
34. Sluiter, A., Hames, B., Ruiz, R., Scarlata, C., Sluiter, J., Templeton, D., 2005. Determination of ash in biomass. Laboratory Analytical Procedure (LAP), NREL/TP-510-42622.
35. Sluiter, A., Hames, B., Hyman, D., Payne, C., Ruiz, R., Scarlata, C., Sluiter, J., Templeton, D., Wolfe, J., 2008a. Determination of total solids in biomass and total dissolved solids in liquid process samples. Laboratory Analytical Procedure (LAP), Technical Report NREL/TP-510-42621.
36. Sluiter, A., Hames, B., Ruiz, R., Scarlata, C., Sluiter, J., Templeton, D., 2008b. Determination of extractives in biomass, Laboratory Analytical Procedure (LAP), Technical Report NREL/TP-510-42619.

37. Sluiter, A., Hames, B., Ruiz, R., Scarlata, C., Sluiter, J., Templeton, D., Crocker, D., 2008c. Determination of structural carbohydrates and lignin in biomass, Laboratory Analytical Procedure (LAP) Technical Report NREL/TP-510-42618.
38. Srinivasan, P., Sarmah, A.K., Smernik, R., Das, O., Farid, M., Gaoc, W., 2015. A feasibility study of agricultural and sewage biomass as biochar, bioenergy and biocomposite feedstock: Production, characterization and potential applications. *Sci. Total. Environ.* 512–513, 495–505.
39. Sun, X.M., Li, Y.D., 2004. Colloidal carbon spheres and their core/shell structures with noble-metal nanoparticles. *Angew. Chem. Int. Ed.* 43, 597–601.
40. Tsilomelekis, G., Orella, M.J., Lin, Z., Cheng, Z., Zheng, W., Nikolakis, V., Vlachos, D.G., 2016. Molecular structure, morphology and growth mechanisms and rates of 5-hydroxymethyl furfural (HMF) derived humins. *Green Chem.* 18, 1983–1993.
41. Tukacs, J.M., Hollo, A.T., Rétfalvi, N., Cséfalvay, E., Dibo, G., Havasi, D., Mika, L.T., 2017. Microwave-assisted valorization of biowastes to levulinic acid. *Chemistry Select.* 2, 1375–1380.
42. Uzuner, S., Cekmecelioglu, D., 2014. Hydrolysis of hazelnut shells as a carbon source for bioprocessing applications and fermentation. *Int. J. Food Eng.* 10, 799–808.
43. van Zandvoort, I., Wang, Y., Rasrendra, C.B., van Eck, E.R.H., Bruijninx, P.C.A., Heeres, H.J., Weckhuysen, B.M., 2013. Formation, molecular structure, and morphology of humins in biomass conversion: influence of feedstock and processing conditions. *ChemSusChem* 6, 1745–1758.
44. Vecchione, L., Moneti, M., Di Carlo, A., Bocci, E., 2015. Biomass waste shell analysis and advanced gasification tests, in: Kao, J.C.M., Sung, W.P., Chen, R. (Eds.), *Green building, materials and civil engineering*. London: CRC Press, Taylor & Francis Group, pp. 55–60.
45. Yates, M., Gomez M.R., Martin-Luengo M.A., ZurdoIbañez V., Martinez Serrano A.M., 2017. MultivalORIZATION of apple pomace towards materials and chemicals. *Waste to wealth. J. Clean.Prod.* 143, 847–853.
46. Xiao, L.-P., Shi, Z.-J., Xu, F. Sun, R.-C., 2012. Hydrothermal carbonization of lignocellulosic biomass. *Bioresour. Technol.* 118, 619–623.
47. Yu, L., Falco, C., Weber, J., White, R.J., Howe, J.Y., Titirici, M.-M., 2012. Carbohydrate-derived hydrothermal carbons: A thorough characterization study. *Langmuir* 28, 12373–12383.

48. Zhang, H., Voroney, R.P., Price, G.W., 2016. Biochar effects on soil organic carbon storage, in: Ok, Y.S., Uchimiya, S.M., Chang, S.X., Bolan, N. (Eds.), Biochar. Production, characterization, and applications. Boca Raton: CRC Press, Taylor & Francis Group, pp. 327-358.

Captions for Figures

Figure 1: Alternative hydrothermal pathways.

Figure 2: Van Krevelen plot of the investigated samples (adapted from (Licursi et al., 2015)).

Figure 3: Thermogravimetric curves of the investigated samples.

Table 1: Compositional analysis of the raw hazelnut shells.

Component		Content (%)	
Cellulose		22.9	
Hemicellulose	Xylose	23.5	18.6
	Arabinose		0.5
	Acetylgroups		4.4
Uronic acids		5.0	
Klasonlignin		37.6	
Ash		1.4	
EtOHextractives		1.4	
Others		8.2	

Table 2: Glucose (GLU), Furfural (FUR), Acetic acid (AA), Levulinic acid (LA), Formic acid (FA) and char yield (wt%) for the one-pot hydrolysis of the hazelnut shells to LA (Path A2 in Figure 1).

Heating system	Exp.	Time (min.)	GLU yield (wt%)	FUR yield (wt%)	AA yield (wt%)	FA yield (wt%)	LA yield (wt%)	(%) of the theoretical LA yield	Hydrochar yield (wt%)
Microwave ^a	MW_1	30	5.1	2.0	10.2	3.7	6.9	42.1	47.0
	MW_2	60	traces	-	10.9	4.4	8.9	54.3	47.8
	MW_3	90	-	-	11.6	4.5	9.2	56.1	47.1
Autoclave ^b	Auto_1	60	5.8	2.4	9.9	3.8	6.7	40.9	43.4
	Auto_2	120	traces	-	8.9	7.8	11.2	68.3	42.7
	Auto_3	180	-	-	6.9	7.6	12.5	76.3	42.6

^a Reaction conditions: hazelnut shells = 2.45 g, water = 35 g, HCl 37 wt% = 1.78 g. Temperature = 180 °C.

^b Reaction conditions: Hazelnut shells = 24.5 g, water = 350 g, HCl 37 wt% = 17.8 g. Temperature = 180 °C.

In depth characterization of valuable char obtained from hydrothermal conversion of hazelnut shells to levulinic acid[#]

Domenico Licursi^a, Claudia Antonetti^a, Sara Fulignati^a, Sandra Vitolo^b, Monica Puccini^b, Erika Ribechini^a, Luca Bernazzani^a, Anna Maria Raspolli Galletti^{a*}

^a Department of Chemistry and Industrial Chemistry, University of Pisa, Via G. Moruzzi 13, 56124, Pisa, Italy. ^b Department of Civil and Industrial Engineering, University of Pisa, Largo Lucio Lazzarino 2, 56122, Pisa, Italy

*Corresponding author: anna.maria.raspolli.galletti@unipi.it

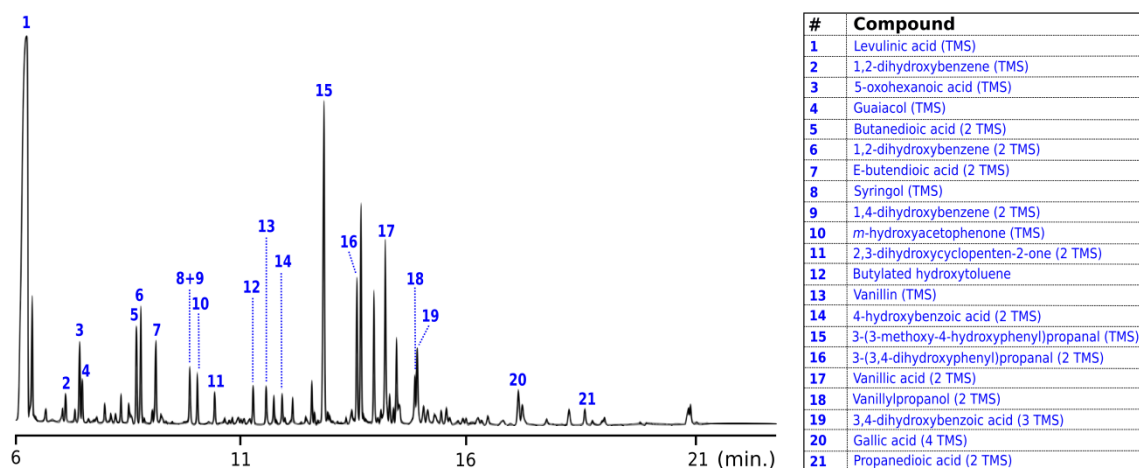


Figure S1: GC-MS analysis of the MW-derived hydrolysate solution.

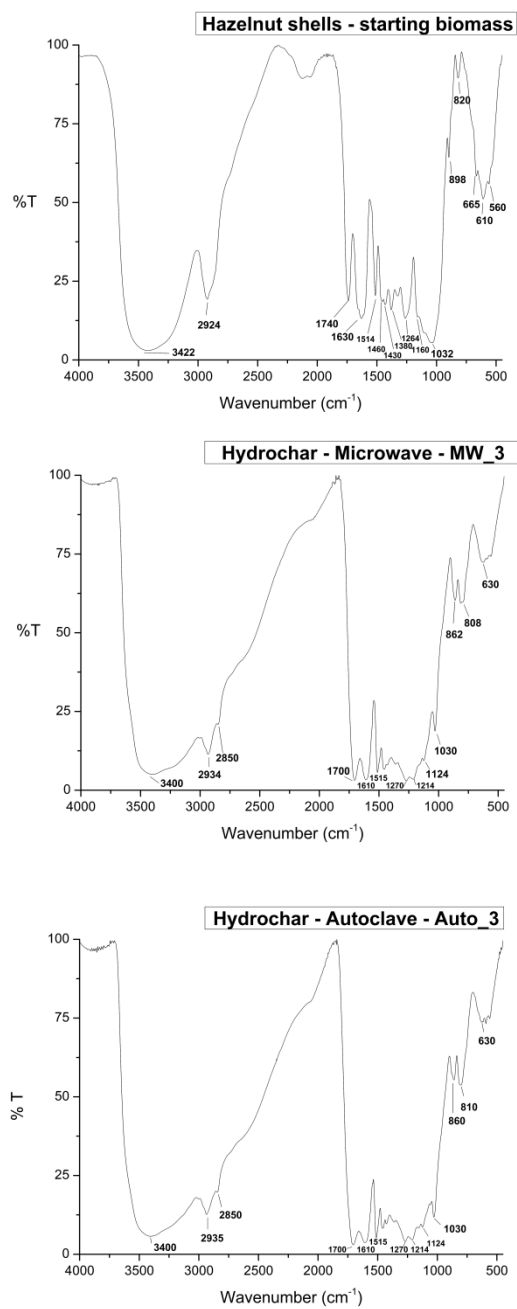


Figure S2: FT-IR spectra of the untreated hazelnut shells and its hydrochars under the optimized reaction conditions in the microwave and autoclave reactor.

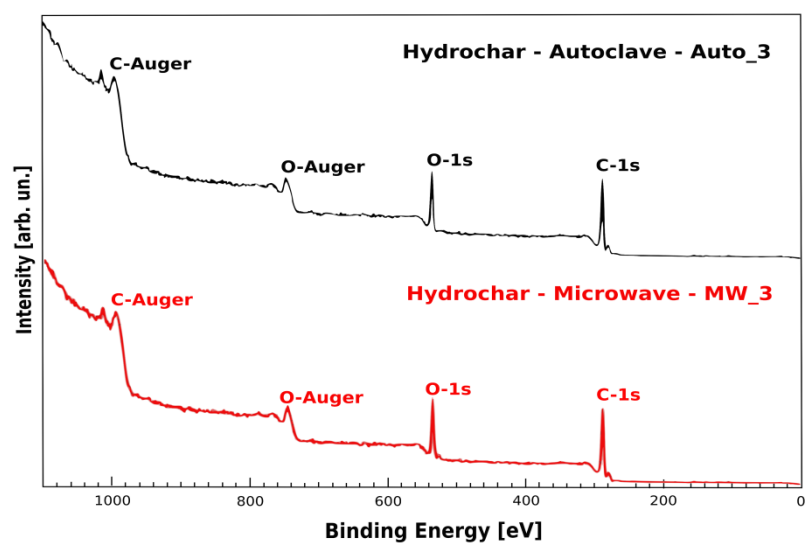


Figure S3: XPS wide-range scanning spectra of the investigated hydrochars.

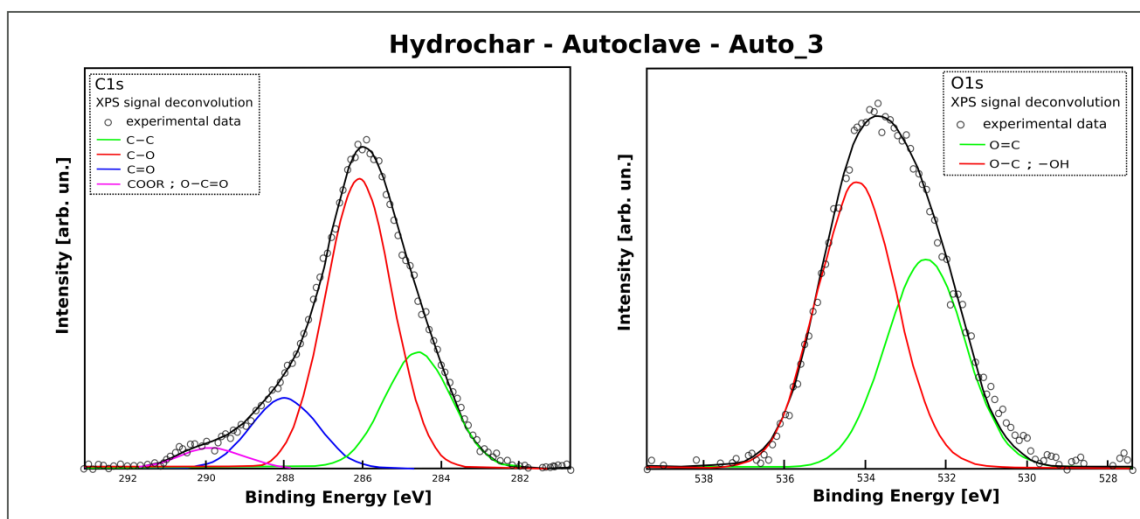


Figure S4: C1s and O1s region scan of the autoclave-hydrochar, along with peak deconvolution.

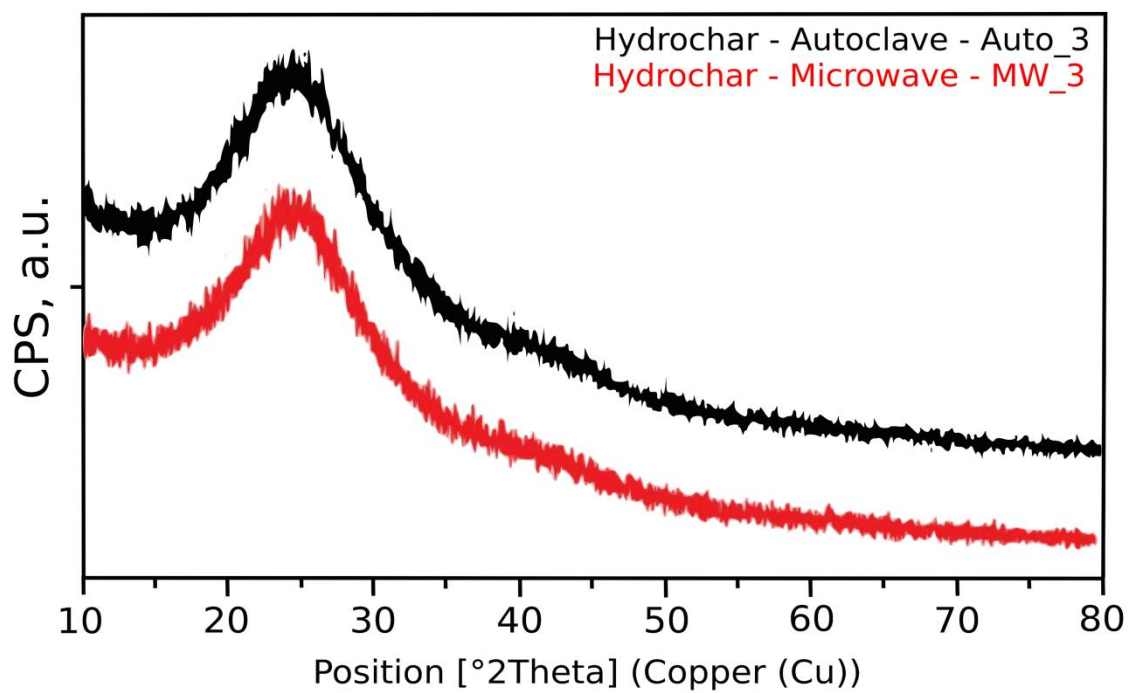


Figure S5: XRD patterns of the synthesized hydrochars.

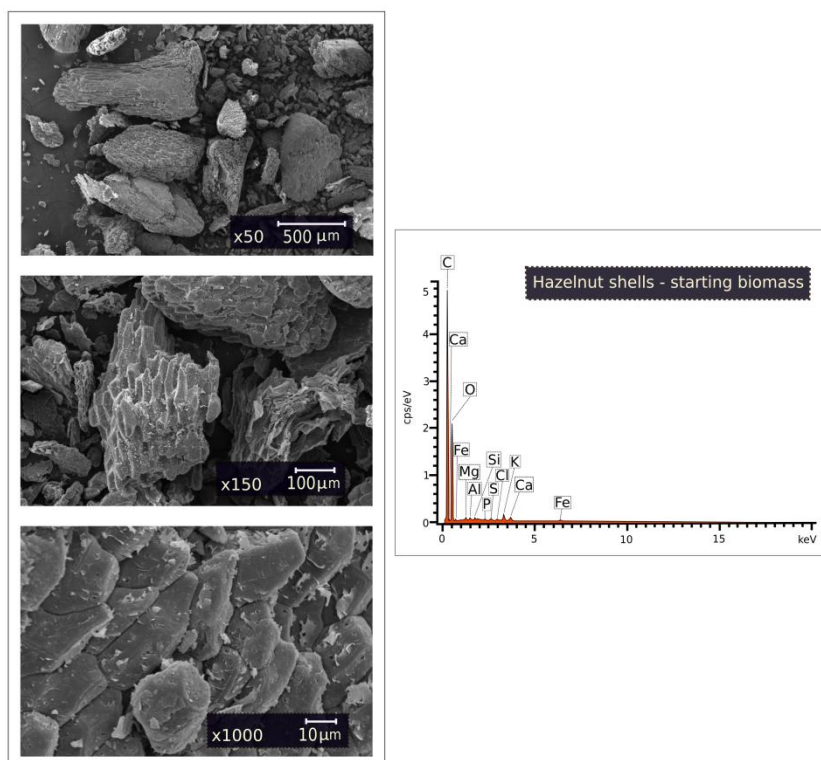


Figure S6: SEM micrographs of the untreated hazelnut shells and EDX spectrum.

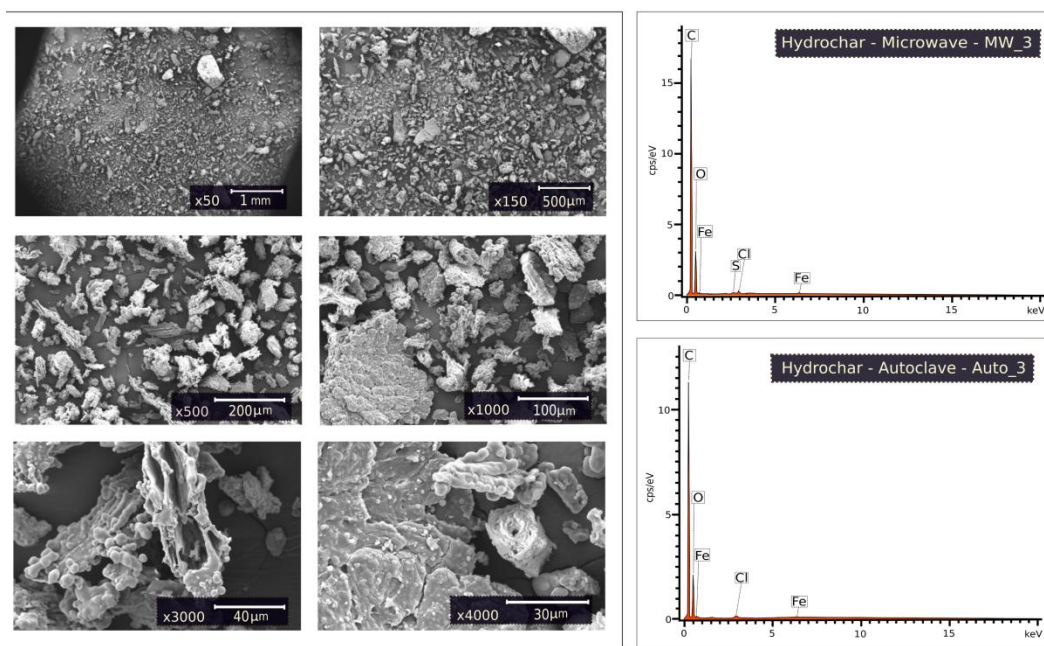


Figure S7: SEM micrographs of the hydrochar recovered after the hydrothermal treatment of the hazelnut shells (Auto_3) and EDX spectra of both hydrochars.